EARTHQUAKE ENGINEERING AND STRUCTURAL DYNAMICS
Earthquake Engng Struct. Dyn. 2000; **29**: 667–682

Flexural–torsional behaviour of steel reinforced concrete members subjected to repeated loading

H-L. Hsu* and C-L. Wang

Department of Civil Engineering, National Central University, Chung-Li 32054, Taiwan

SUMMARY

This paper presents an experimental investigation of the inelastic behaviour of steel reinforced concrete (SRC) members under cyclically applied bending and torsional loading. Fourteen steel reinforced concrete members made from three structural-steel sections with different cross-sectional properties were tested under various combinations of bending and torsion. Results indicate that the ultimate flexural capacity of an SRC member was significantly reduced under a moderate degree of torsion. Based on these findings, a quantitative evaluation of the effect of torsion was made and a simplified interaction curve between bending and torsion is proposed. Copyright © 2000 John Wiley & Sons, Ltd.

KEY WORDS: steel reinforced concrete; earthquake-resistant design; torsion; interaction

1. INTRODUCTION

Steel reinforced concrete (SRC) has been developed over recent decades, and the benefits of using SRC designs include higher carrying capacities for the same member dimensions, better ductility performance than traditional reinforced concrete designs, and higher damping ratios which reduce vibrations due to minor excitation. In general, studying the behaviour of SRC members involves examining steel, concrete, and interaction between them. Research studies [1–6] have shown that interaction between steel and concrete significantly contributes to the performance enhancement of SRC members. However, information currently available on the behaviour of SRC members is limited to their bending, and axial-loading performances or their combinations. Information on the behaviour of these members under torsional loading, which frequently occurs during earthquakes, is still not available.

* Correspondence to: H-L. Hsu, Department of Civil Engineering, National Central University, Chung-Li 32054, Taiwan

Contract/grant sponsor: National Science Council of the Republic of China; Contract/grant numbers: NSC 85-2211-E-008-003 and NSC 86-2211-E-008-014

Received 29 March 1999
Revised 12 August 1999
Accepted 11 November 1999

Copyright © 2000 John Wiley & Sons, Ltd.

When a low-rise building frame is subjected to multi-directional earthquake ground motion, bending and torsional forces are both exerted on most structural members. An experimental study conducted by the present author [7] showed that torsion significantly affected members' bending capacities. This phenomenon also applies to SRC members, since concrete is vulnerable to the shear stress induced by applied torsion. When shear cracks occur in the early stages of loading application, the integrity of structural forms are damaged and SRC member's strength is reduced. Therefore, the behaviour of SRC members under various loading combinations involving torsion should be studied to ensure the adequacy of member performance. Detailed objectives of this study include: (1) conducting experimental investigation of steel reinforced concrete members subjected to combined bending and torsional loading to gather empirical information; (2) evaluating the performance of those members when subjected to coupled loading; and (3) providing a simplified interaction equation for design purpose.

2. EXPERIMENTAL PROGRAM

2.1. Test specimens

Test specimens were fabricated using JIS SS41 structural steel encased in the centres of composite sections. All specimens were 1065 mm high. The steel yield stress was 324.4 MPa. In order to evaluate the effect of sectional aspect ratios during combined loading, three steel sections: $100 \times 100 \times 6 \times 8$, $150 \times 100 \times 6 \times 9$, and $200 \times 100 \times 5.5 \times 8$ mm, were used. The three test-sample series were designated SRC(1), SRC(2), and SRC(3). Detailed dimensions and steel- bar-reinforcement layout are shown in Figure 1. The two ends of the specimen were welded to 25-mm-thick end plates. Six bolt holes were drilled in each end plate so the tops of specimens could be bolted to a loading beam and their bottoms fixed to a test platform fastened to a strong floor.

The reinforced concrete was composed of $\#4$ longitudinal bars and $\#3$ stirrups on 150 mm spacing. Longitudinal reinforcing bars were attached to both end plates using all-around welds to reflect accurately the boundary continuity conditions. Rectangular confined concrete areas were thus formed by this arrangement. The shorter and longer dimensions of the rectangles bounded by the centrelines of the outermost closed transverse reinforcements, as shown in Figure 1, were designated x_0 and y_0 , respectively. The yield stresses for the $\#3$ and $\#4$ deformed bars were 372.7 and 312.2 MPa, respectively. The average compressive strength of the concrete used to fabricated the specimens was 27.7 MPa, as determined by cylinder testing after a 28-day curing process. In order to ensure uniform transmission of applied loads to the reinforced concrete, four shear studs were welded to each end plate. Stresses induced on the steel sections and the steel bars were measured by installed strain gauges. Strains on the centres and edges of flanges were measured to evaluate the magnitude of warping stresses induced by applied torsional loading.

2.2. Test set-up

The test program was conducted in the Structural Engineering Laboratory of National Central University, which has a 10-m-wide, 50-m-long strong-floor testing zone and four 7-m-high reaction walls. Test platform was first fastened to the strong floor using anchor bolts. Test specimens were bolted to the platform with six A325 high-strength bolts. A 3.5 m stiffened loading beam linked to two servo-controlled actuators (one for bending and one for torsion) to transmit

Copyright © 2000 John Wiley & Sons, Ltd

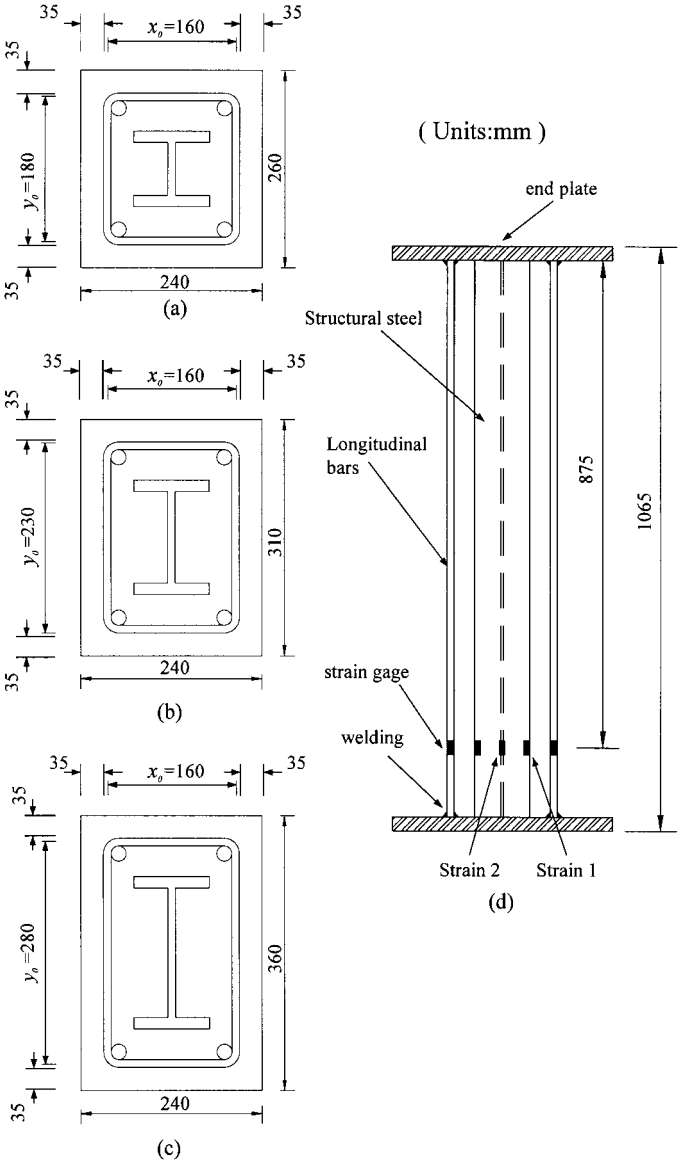

Figure 1. Description of specimens: (a) SRC(1) with H100 × 100 × 6 × 8 steel section; (b) SRC(2) with H150 × 100 × 6 × 9 steel section; (c) SRC(3) with H200 × 100 × 5.5 × 8 steel section; (d) vertical dimensions of specimens and placements of strain gages.

loads was placed atop specimens. The capacities of the actuators used to generate bending and torsion were 1000 and 250 kN, respectively.

The larger actuator was placed at the centre of the loading beam to generate bending moment, and the small actuator was attached to one end of the loading beam; the distance

Copyright © 2000 John Wiley & Sons, Ltd

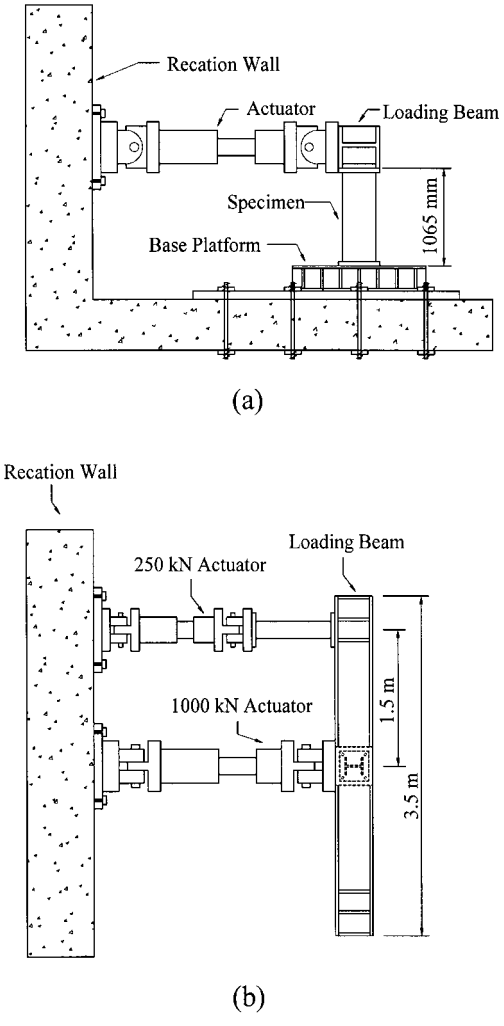

Figure 2. Test setup: (a) side view; (b) top view.

between the actuators was 1.5 m. Actuator piston movements were controlled by function generators. The plan and elevation dimensions of specimens and loading set-up are shown in Figure 2.

2.3. *Test procedures*

Test loadings included pure bending, pure torsion, and combined cyclic bending and torsion. Pure bending was generated by driving both actuators with same displacement commands, as

Copyright © 2000 John Wiley & Sons, Ltd

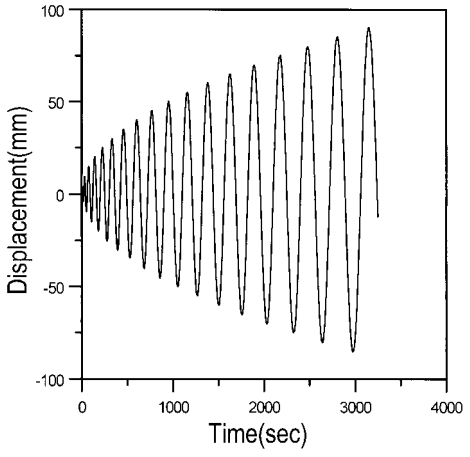

Figure 3. Displacement commands.

Table I. Interaction between normalized bending and torsional strength.

Specimen	Loading combination	Bending strength (kN-m)	Normalized torsion (T/T_u)	Normalized bending strength (M/M_u)
SRC(1)-1	Pure bending	65.2	0	1
SRC(1)-3	Bending + $0.225T_u$	61.6	0.225	0.945
SRC(1)-4	Bending + $0.45T_u$	55.4	0.45	0.850
SRC(1)-5	Pure torsion	—	1	0
SRC(2)-1	Pure bending	104.4	0	1
SRC(2)-2	Bending + $0.11T_u$	100.5	0.11	0.963
SRC(2)-3	Bending + $0.225T_u$	83.9	0.225	0.804
SRC(2)-4	Bending + $0.45T_u$	82.4	0.45	0.789
SRC(2)-5	Pure torsion	—	1	0
SRC(3)-1	Bending	137.5	0	1
SRC(3)-2	Bending + $0.11T_u$	133.3	0.11	0.969
SRC(3)-3	Bending + $0.225T_u$	118.6	0.225	0.863
SRC(3)-4	Bending + $0.45T_u$	99.8	0.45	0.726
SRC(3)-5	Pure torsion	—	1	0

Notes: 1. M_u: bending strength of member subjected to pure bending.
2. T_u: torsional strength of member subjected to pure torsion.

shown in Figure 3. Pure torsion was generated by fixing the centre actuator in place and monotonically exerting pulling force with the smaller actuator attached to the end of the loading beam. Strengths of test specimens obtained from pure bending and pure torsion tests were used as a base for comparison.

Copyright © 2000 John Wiley & Sons, Ltd

In order to investigate the effect of torsion on the reduction of a member's bending capacity, a series of combined loading tests using different levels of applied torsion were conducted. For the combined loading test, the larger actuator which generated bending moment was driven by prescribed cyclic displacement commands, while the smaller actuator was operated under force control so that a constant torsion could be maintained. The amplitude increment for the larger actuator was 5 mm per half-cycle until the member reached its maximum strength. Specimens were labeled according to the applied loading. For examples, SRC(1)-1, SRC(2)-1, and SRC(3)-1 indicate members tested under pure bending; while SRC(1)-5, SRC(2)-5, and SRC(3)-5 represent

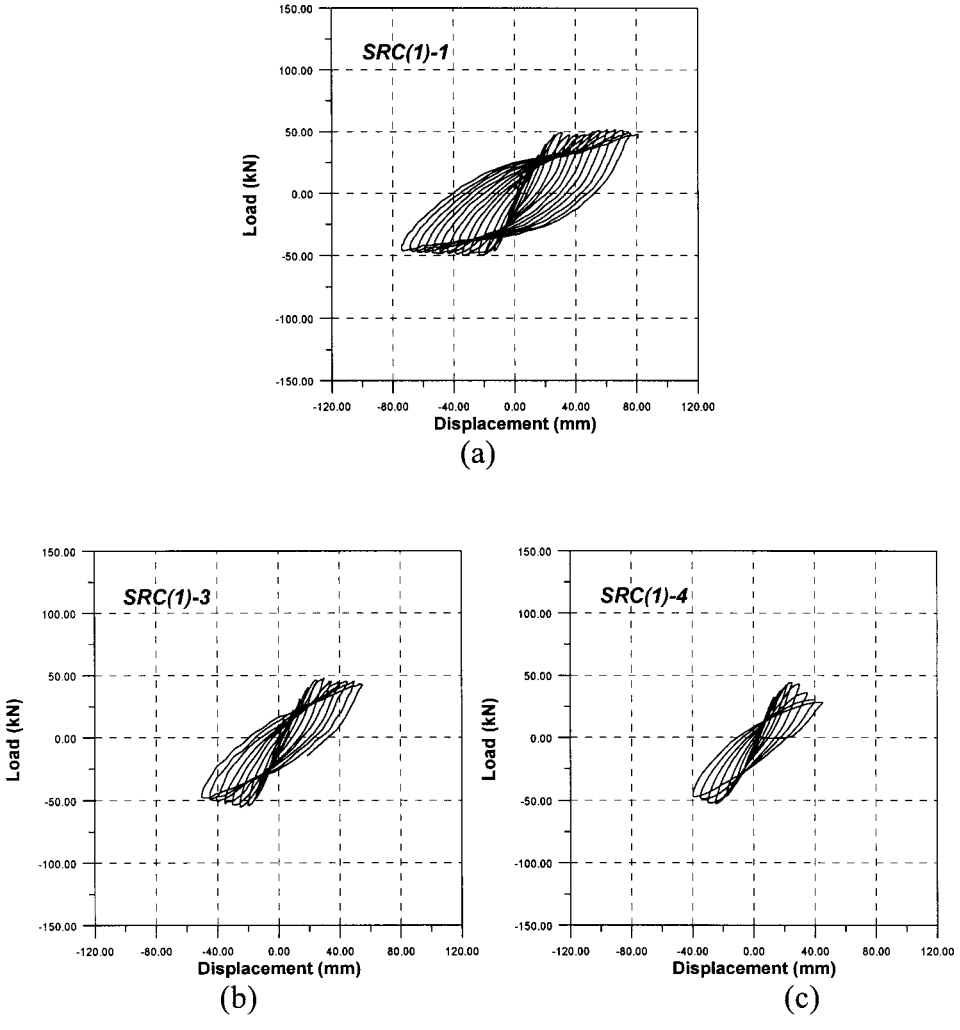

Figure 4. Hysteretic curves: (a) SRC(1)-1; (b) SRC(1)-3; (c) SRC(1)-4; (d) SRC(2)-1; (e) SRC(2)-2; (f) SRC(2)-3; (g) SRC(2)-4; (h) SRC(3)-1; (i) SRC(3)-2; (j) SRC(3)-3; (k) SRC(3)-4.

Copyright © 2000 John Wiley & Sons, Ltd

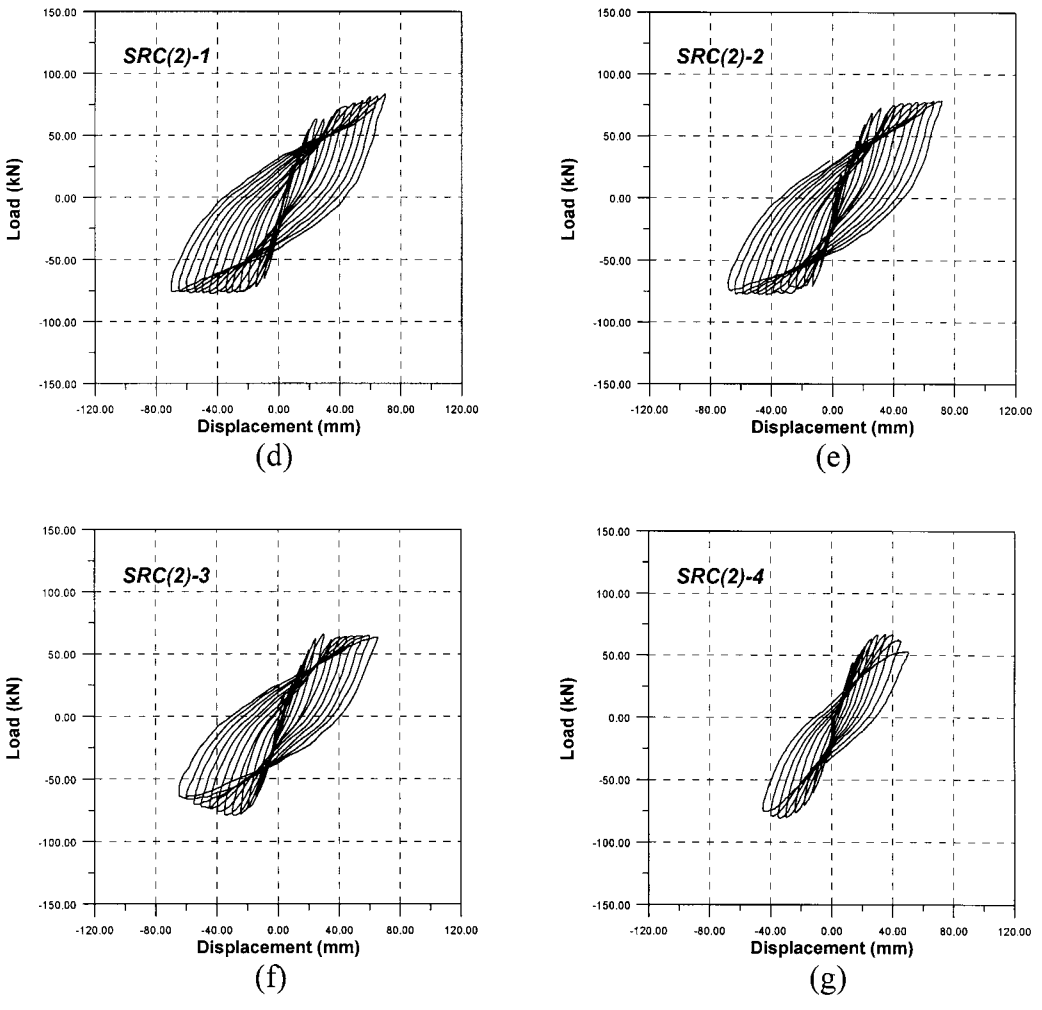

Figure 4. Continued.

members subjected to pure torsion. Detailed loading combinations for the test specimens are shown in Table I. Hysteretic curves for specimens subjected to repeated loading are shown in Figure 4. Relationships between torsion and twist angle for members subjected to pure torsion are shown in Figure 5.

3. FAILURE MECHANISM

3.1. Pure bending

Specimen tested under pure bending began exhibiting at the bottoms of cracks on their front and back sides, which had been subjected to the maximum tensile stresses. Cracks then appeared on

Copyright © 2000 John Wiley & Sons, Ltd

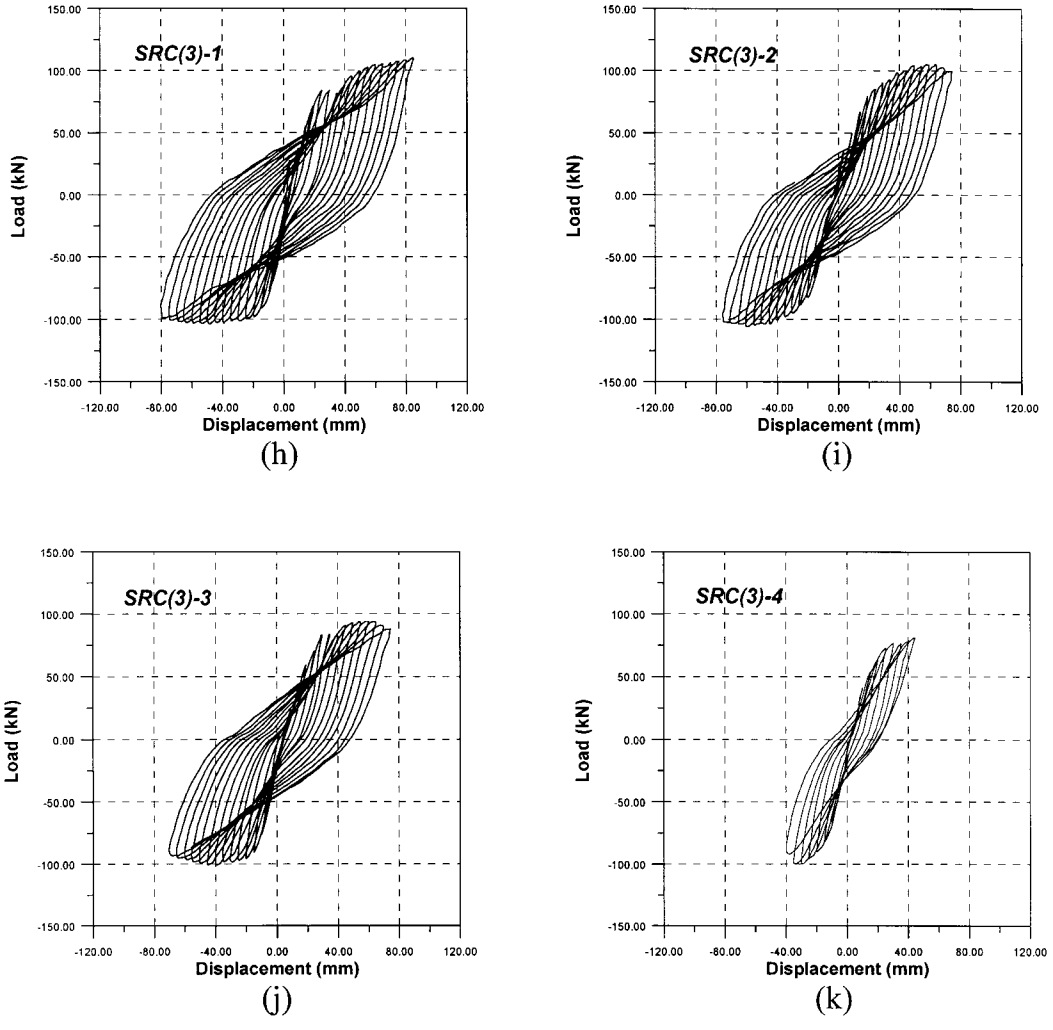

Figure 4. Continued.

both sides of members and progressively spread upwards as displacement of the tops of the specimens was increased. The longitudinal steel bars reached the buckling stage when crack zones spread upwards far enough to cause crushing of the concrete. Failure mode was characterized as appearance of tensile cracks, buckling of longitudinal bars and crushing of concrete blocks. Ultimate bending strengths obtained from the pure bending tests were designated M_u and used for later comparisons.

3.2. Pure torsion

Significant diagonal cracks resulting from shear stresses were observed at the centres of specimens when torsion was first applied. The cracks widened when twist angles were increased. The

Copyright © 2000 John Wiley & Sons, Ltd

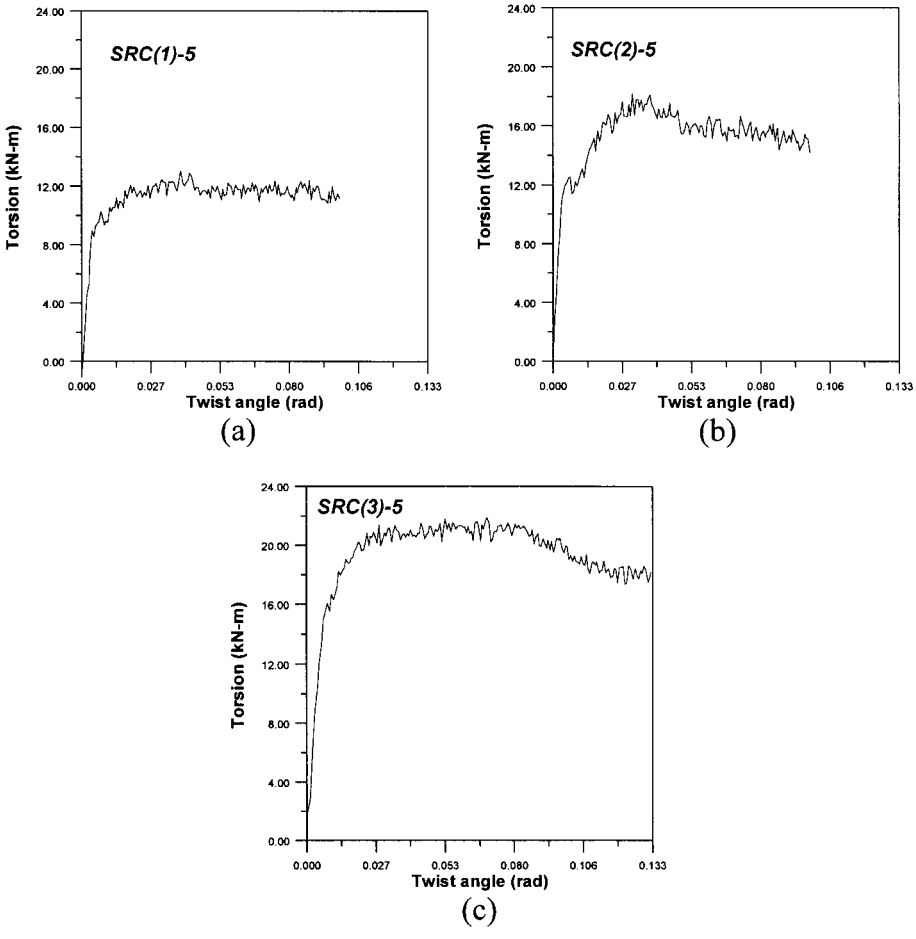

Figure 5. Relationship between torsion and twist angle for members subjected to pure torsion: (a) SRC(1)-5; (b) SRC(2)-5; (c) SRC(3)-5.

diagonal cracks spread to both ends of specimens as the test progressed, and in the final stage, longitudinal cracks appeared adding to and combining with the growth of the existing diagonal cracks. Maximum torsional strength, designated T_u, was reached when the concrete crumbled due to cumulative cracking. The T_u values for the three specimens tested under pure torsion are listed in Table II. Failure modes of members subjected to pure torsion are also shown in Figure 6.

3.3. Combined bending and torsion

Failure mechanisms of members subjected to combined bending and torsion started with the appearance of flexural cracks at the bottoms of the specimens. Diagonal shear cracks were then observed when the torsional strength of cracked section was lower than the applied torsional force. Failure of specimens occurred due to combinations of shear and flexural cracks. It was

Copyright © 2000 John Wiley & Sons, Ltd

Table II. Torsional strength of SRC members.

Specimen	T_{RC} (kN-m)	T_S (kN-m)	T_W (kN-m)	T_W/T_S	T_{SRC} (kN-m) (Equation (8))	T_u (kN-m)	T_u/T_{SRC}
SRC(1)	8.5	1.43	0.31	0.22	10.24	13.1	1.28
SRC(2)	10.8	1.90	0.43	0.23	13.13	17.1	1.30
SRC(3)	13.2	1.66	0.54	0.33	15.4	20.5	1.33

Note: 1. T_{RC} :Torsional strength of reinforced concrete.
2. T_S: St. Venant torsion of steel section.
3. T_W: Warping torsion of steel section.
4. T_{SRC}: Torsional strength of SRC section.
5. T_u: Torsional strength measured from tests.

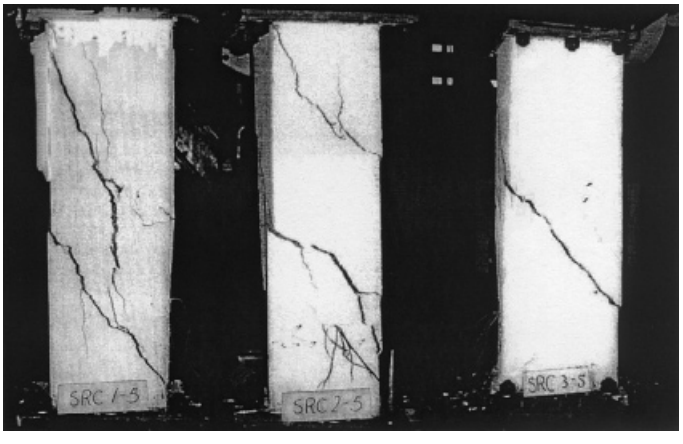

Figure 6. Failure modes of members subjected to pure torsion.

observed during testing that concrete crack zones increased as the magnitude of applied torsion was increased, thus significantly reducing the member's bending capacity. A comparison of bending strengths for all test specimens is also listed in Table I. Failure modes of members subjected to combined loading are shown in Figure 7.

4. COMPARISON AND INTERPRETATION OF TEST DATA

4.1. General comparison

In order to determine the influence of torsion on members' bending strength, a comparison of test results between members subjected to and not subjected to torsion was made. In each test series, the ultimate bending strength of members subjected to combined loading (M) was normalized with respect to that of the member subjected to pure bending alone (M_u).

Copyright © 2000 John Wiley & Sons, Ltd

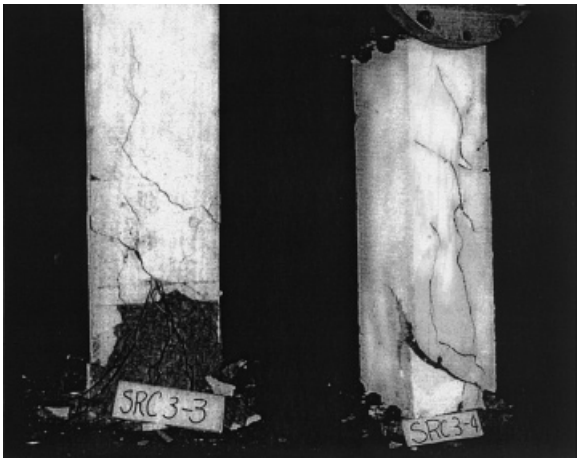

Figure 7. Failure modes of members subjected to combined loading.

The comparison given in Table I shows that effect of minor torsion ($0.11T_u$) on the members' bending capacity was minimal and that all members maintained at least 96 per cent of their bending strengths. However, members subjected to medium to high degrees of torsion exhibited significant reductions in their bending capacities. In the SRC(1) test series, for example, specimens made of $H100 \times 100 \times 6 \times 8$ encased steel experienced a maximum 15 per cent reduction in bending strength when members were simultaneously subjected to 45 per cent of their torsional strength ($0.45T_u$). Similarly, in SRC(3) test series, specimens made of $H200 \times 100 \times 5.5 \times 8$ encased steel sustained a larger strength reduction of 27 per cent when members were also subjected to 45 per cent of their torsional strength.

The interaction between normalized bending strength and normalized torsion for the three sections tested is shown in Figure 8, and can be linearly approximated as follows:

$$\frac{M}{M_u} + R\frac{T}{T_u} = 1 \tag{1}$$

in which M and T represent allowable bending moment and torsion under combined loading, respectively, and R is a factor accounting for the effect of torsion in reducing members' bending strength.

Specifically, the interaction between bending and torsion for the three test series can be quantified as follows:

$$\mathrm{SRC}(1)\left(\frac{y_0}{x_0} = 1.13\right): \frac{M}{M_u} + 0.335\,\frac{T}{T_u} = 1 \tag{2}$$

$$\mathrm{SRC}(2)\left(\frac{y_0}{x_0} = 1.44\right): \frac{M}{M_u} + 0.478\,\frac{T}{T_u} = 1 \tag{3}$$

$$\mathrm{SRC}(3)\left(\frac{y_0}{x_0} = 1.75\right): \frac{M}{M_u} + 0.639\,\frac{T}{T_u} = 1 \tag{4}$$

Copyright © 2000 John Wiley & Sons, Ltd

Equations (2)–(4) show that the effect of torsion on reducing bending capacity is closely related to the aspect ratios of the confined concrete (y_0/x_0). For example, test series SRC(3) possessed a y_0/x_0 ratio of 1.75, and its reduction in bending strength due to torsion was 1.9 times that of the SRC(1) test series, which possessed a lower y_0/x_0 ratio of 1.13.

4.2. Torsional strength of steel reinforced concrete

According to ACI [8], the torsional moment strength of a rectangular reinforced concrete section (T_{RC}), as shown in Figure 9, can be calculated as follows:

$$T_{RC} = \frac{2A_0 A_t F_{yv} \cot\theta}{S} \tag{5}$$

in which F_{yv} is the yield strength of the transverse reinforcement, S is the spacing of the transverse reinforcements, θ is the angle of compression diagonal, which can be assumed as 45° for non-prestressed reinforced concrete members, A_t is the area of transverse reinforcement, A_o is the area enclosed by the shear flow path and can be simplified to 85 per cent of the area enclosed by the centreline of the outermost enclosed transverse reinforcement (A_{oh}), which can be expressed as follows:

$$A_{0h} = x_0 y_0 \tag{6}$$

The torsional strength of a structural steel section can be attributed to uniform St. Venant torsion and non-uniform warping torsion. The fully plastic torque of a structural steel section due to St. Venant shear, T_S, can be calculated as [9]

$$T_s = \tau_y \left[t_f^2 \left(b_f - \frac{t_f}{3} \right) + \frac{t_w^2}{2} \left(d + \frac{t_w}{3} \right) - t_f t_w^2 \right] \tag{7}$$

In Equation (7), the τ_y of the structural steel section used to fabricate specimens is equal to 187.3 MPa, b_f is the width of the flange, d is the depth of the section, t_f and t_w are the respective thicknesses of the flange and the web. For steel section encased in concrete, the warping effect is complicated and is affected by concrete confinement. Therefore, the warping torsion can be more accurately acquired using measured warping strains. The strains due to warping on the steel section flanges of the three specimens tested under pure torsion are shown in Figure 10. The corresponding warping torsions of the test specimens, T_w, were approximately 22–33 per cents of the steel sections' St. Venant torsions when T_u was reached. The torsional strength of an SRC member (T_{SRC}) can thus be approximated by summing the torsional strengths of the reinforced concrete and the structural steel:

$$T_{SRC} = T_S + T_w + T_{RC} \tag{8}$$

Table II shows the measured strength and calculated strength according to ACI. It can be found that the ratios between measured values and calculated values fall between 1.28 and 1.33. These ratios actually reflect safety factor differences between ultimate strength and nominal strength. A minimal value 1.28 can be used for design purpose.

Further comparison of the component torsional strengths of the steel sections and reinforced concrete of the SRC sections listed in Table II shows that the reinforced concrete contributed major torsional strength. When the concrete cracked, the overall torsional strength of the composite section decreased significantly. Therefore, the parameter most strongly affecting the

Copyright © 2000 John Wiley & Sons, Ltd

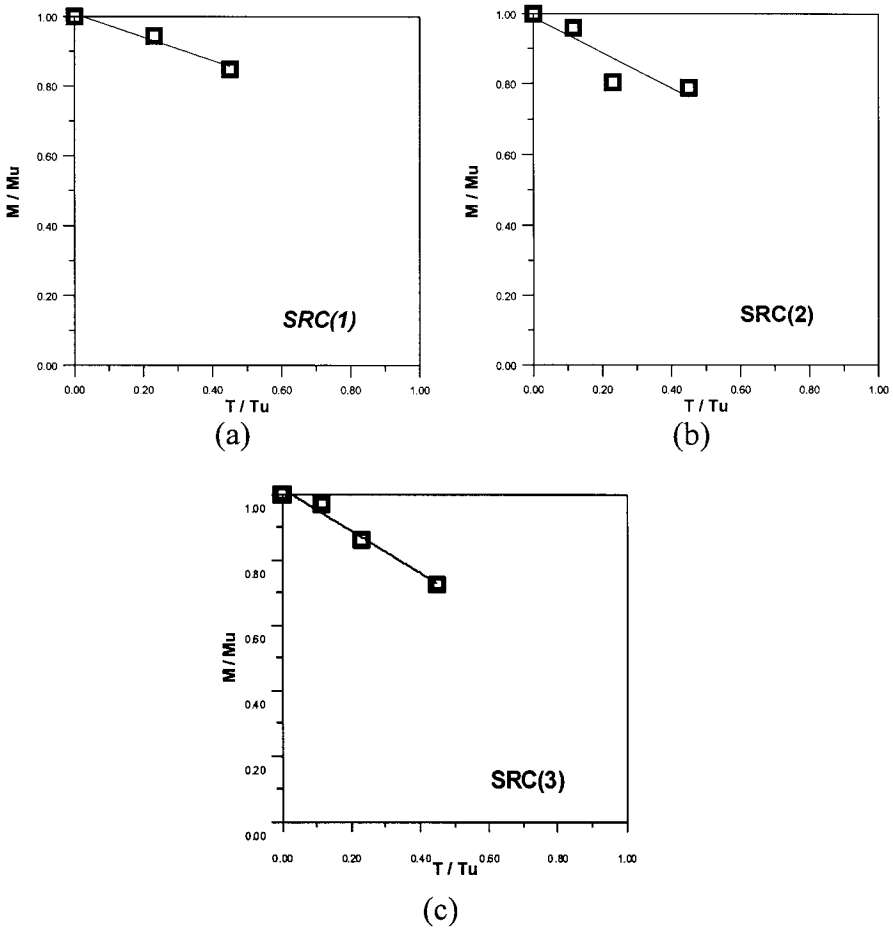

Figure 8. Interaction curves for members subjected to combined bending and torsion: (a) SRC(1) test series; (b) SRC(2) test series; (c) SRC(3) test series.

torsional effect factor R in Equation (1) is the dimension of the confined reinforced concrete, specifically, A_{oh}, since the torsional resistance of a rectangular reinforced concrete section is governed by its confined concrete area. As shown in Equations (2)–(4), an increase in y_0/x_0 ratio results in a higher torsional effect factor R, therefore, the dimensions x_0, y_0 must be adjusted appropriately to maximize the torsional resistance of composite sections.

Plotting the relationship between the torsion effect factor R and the aspect ratios of the confined reinforced concrete sections (y_0/x_0) as shown in Figure 11 shows that these two parameters can be linearly approximated as

$$R = 0.49\left(\frac{y_0}{x_0}\right) - 0.22 \tag{9}$$

Copyright © 2000 John Wiley & Sons, Ltd

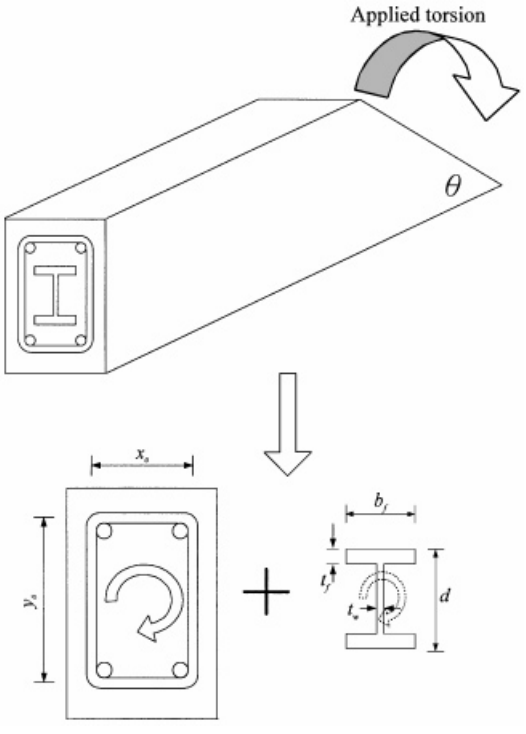

Figure 9. Definition of SRC section subjected to torsion.

Therefore, the interaction between bending and torsion for a steel reinforced concrete member can be simplified to

$$\frac{M}{M_u} + \left\{0.49\,\frac{y_0}{x_0} - 0.22\right\}\left(\frac{T}{T_u}\right) = 1 \tag{10}$$

This equation provides adequate accuracy for estimating the flexural–torsional behaviour of SRC members with confined concrete aspect ratios less than 1.75.

5. SUMMARY AND CONCLUSION

This paper reports test results for 14 SRC members with three different encased structural-steel section configurations subjected to combined bending and torsion. It is shown that the composite sections were vulnerable to torsional loading. Major reductions in bending strength (approximately 27 per cent in the SRC(3) test series) were exhibited when moderate degrees of torsion were applied (approximately 45 per cent of member's torsional strength). Therefore, the effect of torsion must be carefully taken into account when calculating the strength of SRC members that

Copyright © 2000 John Wiley & Sons, Ltd

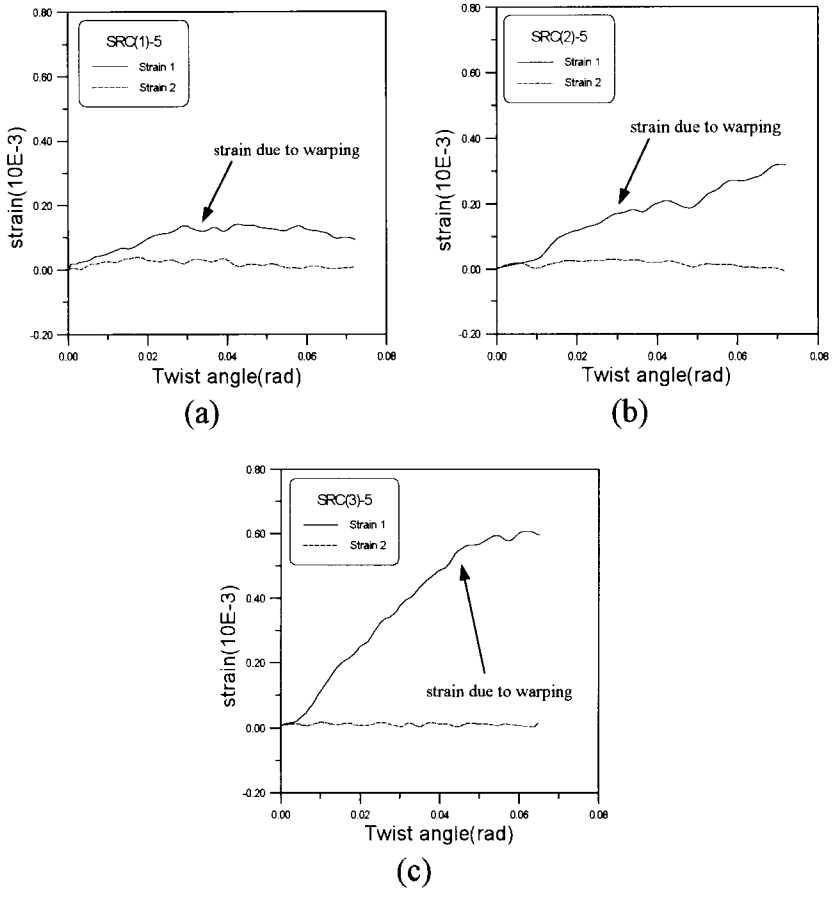

Figure 10. Strains due to warping on the flanges of steel sections: (a) SRC(1)-5; (b) SRC(2)-5; (c) SRC(3)-5.

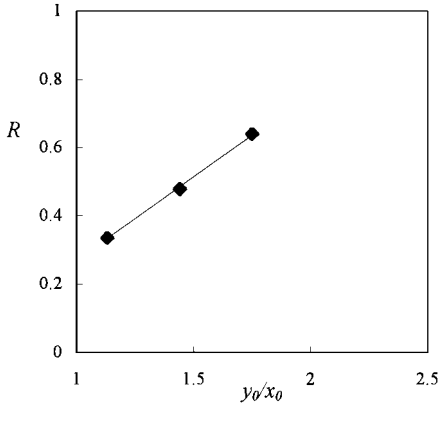

Figure 11. Relationship between torsion effect factor and aspect ratios of confined concrete.

Copyright © 2000 John Wiley & Sons, Ltd

may be subjected to earthquake-induced loading. Comparison of the test data also demonstrates that the effect of torsion on reducing members' bending strengths is more significant for members with larger aspect ratios. Accordingly, a simplified interaction equation between bending and torsion has been proposed for design purposes.

ACKNOWLEDGEMENTS

This study was partially supported by the National Science Council of the Republic of China under Grant No. NSC 85-2211–E-008-003 and NSC86-2211-E-008-014, which is gratefully acknowledged.

REFERENCES

1. Boyd PF, Cofer WF, McLean DI. Seismic performance of steel-encased concrete columns under flexural loading. *ACI Structural Journal* 1995; **92**(3):355–364.
2. Furlong RW. Design of steel-encased concrete beam-columns. *Journal of Structural Engineering* 1968; **94**(1):267–281.
3. Mirza SA, Skrebek BW. Reliability of short composite beam-column strength interaction. *Journal of Structural Engineering* 1991; **117**(8):2320–2339.
4. Naka T, Morita K, Tachibana M. Strength and hysteretic characteristics of steel-reinforced concrete columns (Part 2). *Transactions of AIJ* 1977; **250**:47–58.
5. Ricles JM, Paboojian S. Seismic performance of steel-encased composite column. *Journal of Structural Engineering* 1994; **120**(8):2474–2494.
6. Wakabayashi M. A proposal for design formulas of composite columns and beam-columns. Proceedings of the Second Insternational Colloquim on Stability, Tokyo, Japan, 1976; 65–87.
7. Hsu HL. Experimental study of performance of structural steel members subjected to multi-dimensional ground motion. International Conference on Computational Methods and Testing for Engineering Integrity, Kuala Lumpur, Malaysia, 1996; 187–196.
8. ACI, *Buildings Code Requirements for Structural Concrete* (*ACI* 318-95). American Concrete Institute: Detroit, MI, 1995.
9. Boresi AP, Sidebottom MO. *Advanced Mechanics of Materials*, (4th edn). Wiley: New York, 1985.

Copyright © 2000 John Wiley & Sons, Ltd